Electronic supplementary information

A Centimeter Scale Self-Standing Two-Dimensional Single-Layered Mesoporous Platinum Nanosheets

Yunqi Li [a, b], Yuwei Liu[a, b], Jing Li[a, b], Danping Xiong[a, b], Xiran Chen[a, b], Mingtao Liu[a, b], Zhong Zheng[a, b], Victor Malgras[d], Yoshio Bando[d], Yusuke Yamauchi[c*] and Jun Xu[e, f*]

[a] *Department of Automotive Engineering, School of Transportation Science and Engineering, Beihang University, Beijing, 100191 China.*

[b] *Vehicle Energy & Safety Laboratory (VESL), Beihang University, Beijing, 100191, China.*

[c] *School of Chemical Engineering and Australian Institute for Bioengineering and Nanotechnology (AIBN), The University of Queensland, Brisbane, Queensland 4072, Australia.*

[d] *WPI Center for Materials Nanoarchitectonics (MANA) and International Center for Young Scientists (ICYS), National Institute for Materials Science (NIMS), Tsukuba, 3050044, Japan.*

[e] *Department of Mechanical Engineering and Engineering Science, The University of North Carolina at Charlotte, Charlotte, NC 28223, USA.*

[f] *Vehicle Energy & Safety Laboratory (VESL), North Carolina Motorsports and Automotive Research Center, The University of North Carolina at Charlotte, Charlotte, NC 28223, USA.*

E-mail: Bando.Yoshio@nims.go.jp, jun.xu@uncc.edu, Yamauchi. Yusuke@nims.go.jp

Experimental

Chemicals and materials

Triblock copolymers poly(styrene-b-2-vinyl pyridine-b-ethylene oxide) PS_{192}-b-$P2VP_{143}$-b-PEO_{613} (subscript represents the number of each unit) was purchased from Polymer Source (Canada). Methanol (CH_3OH), tetrahydrofuran (THF), Nickel(II) chloride hexahydrate and dimethylaminobenzaldehyde (DMAB) were obtained from Acros Organics (Belgium). Dihydrogen hexachloroplatinate(IV) hexahydrate ($H_2PtCl_6 \cdot H_2O$), commercially available Pt black, ascorbic acid (AA) and commercial Pt/C catalyst (20 wt% Pt) used here were obtained from Alfa Aesar (UK). 5 wt% Nafion solution was purchased from Sigma Aldrich (USA). 35% hydrochloric acid (HCl) and sulfuric acid (H_2SO_4) were purchased from Beijing chemical plant (China). Perchloric acid was obtained from Aladdin (China).

Synthesis of meso-Pt NSs and meso-PtNi NSs

The micelle solution was prepared first. 10 mg of triblock copolymer PS_{192}-b-$P2VP_{143}$-b-PEO_{613} was completely dissolved in 5 mL of THF, and ultrasonic wave cleaner was used to accelerate its dissolution. Then, 100 μL of 35% HCl was added and the solution was magnetically stirred for 10 min to stimulate micellization. The obtained solution was transferred into a dialysis membrane tube (Mw cut-off: 14,000 Da) and was dialyzed against methanol for six dialysis cycles. Each cycle took 6 h to completely remove the THF. Finally, a 25 mL volumetric flask was used to set micelle capacity with a concentration of 0.4 $g \cdot L^{-1}$, and the pH of the polymer micelle solution was adjusted to 3 by adding an appropriate amount of 35% HCl solution.

Bare silicon wafers were cut into square sheets of 15×15 mm, rinsed with ethanol, and dried for further use. 1 mL of the polymeric micelle solution (0.4 $g \cdot L^{-1}$) was mixed with 92.3 μL of 200 mM H_2PtCl_6 solution and stirred for 30 min at room temperature. 112 μL of the mixture was

deposited onto silicon substrates via spin coating (500 rpm, 10s and 1000 rpm, 20 s). The silicon wafers were dried in a chamber at room temperature for 15 min. After that, another 112 μL of composite solution was spin-coated onto the silicon substrates under the same conditions as above. Until solvent evaporation, the silicon substrates with a small amount of DMAB powders were placed in a closed vessel at 28 °C for a day. For further reduction, the silicon substrates were immersed in 0.1 M aqueous solution of ascorbic acid for 10 min. Then the substrates were calcined for an hour at 350 °C until the thin films on the substrates completely dried. After put the silicon substrates into 3 M NaOH solution for 24 h, the solid black Pt powder were collected and rinsed 3 to 5 times by deionized water and centrifuged with a centrifuge. The final black products were obtained and kept for further characterization. The preparation of meso-PtNi NSs was following the same method to the synthesis of meso-Pt NSs with 23.1 μL of 200 mM $NiCl_2$ solution as Ni precursor.

Different sizes of catalyst film can be prepared by adjusting the size of the silicon wafer. Before separating the meso-Pt NSs from the silicon wafer substrate, 50 μL of 30% Nafion solution was added dropwise on the surface of the catalyst. The volume of the Nafion solution is proportional to the area of the catalyst film. After the Nafion solution was completely dried, immersing the substrate into 3M NaOH solution to separate the catalyst film from the substrate, and then the film was rinsed in deionized water.

Characterization

Field emission scanning electron microscope (SEM, HITACHI S-4800, Japan) was operated to observe morphology of meso-Pt NSs at 10 kV. Transmission electron microscope (TEM, JEOL JEM-2200F, Japan) was employed to confirm the internal structure at 120 kV. Furthermore, scanning transmission electron microscopy (STEM, JEOL JEM-2200F, Japan) image and elemental mapping were obtained in the high angle annular dark field (HAADF) mode. Wide-angle X-ray diffraction (XRD, RIGAKU, Japan) was used to determine the phase composition. The X-ray photoelectron spectroscopy (XPS) analysis was conducted by using a Kratos AXIS SUPRA spectrometer. The thermal stability of the composites was measured under a themogravimetric analysis (TG, TA instruments Q600 SDT, USA). The morphology of the micelles and meso-Pt NSs were performed using atomic force microscope (AFM, Bruker, USA) with the non-contact mode.

Electrochemical Measurements

Electrochemical measurements were performed in a conventional three-electrode cell, including Ag/AgCl (Saturated KCl) as the reference electrode and platinum wire as the counter electrode, by using a CHI 750E electrochemical analyzer (CHI Instruments. USA).

As for ORR measurements, a rotating ring-disk electrode (RRDE) (4 mm in diameter) was as the working electrode. Typically, 5 mg of catalyst was dispersed in 1 mL of 1:2 (v/v) isopropanol/water mixed solvent (containing 0.05 mL of 5.0 wt% Nafion solution) under sonication for at least 30 min to form a homogenous catalyst ink. Then, 5 μL of the electrocatalyst ink was dropped on the surface of a glassy carbon (GC) electrode. The ORR evaluation was performed by using RRDE-3A rotation system (ALS Co. Ltd, Japan). Linear sweep voltammetry (LSV) measurements were obtained in O_2-saturated 0.1 M $HClO_4$ solution with the potential range between 0.056 V and 1.256 V (vs. reversible hydrogen electrode (RHE)), at a scan rate of 10 mV s-1 and a typical rotation speed of 1600 rpm. Durability tests of the meso-PtNi NSs and Pt/C catalysts were carried out according to the accelerated durability test protocol by cycling the catalysts between 0.6 and 1.0 V in O_2-saturated 0.1 M $HClO_4$ at a scan rate of 50 mV s^{-1}.

As for MOR measurements, the working electrode was a glassy carbon electrode (GCE)

modified with 3 μL of catalyst dispersion (5mg mL^{-1}), then 3 μL of 0.25 wt.% Nafion aqueous solution were coated on top and dried. Cyclic voltammograms (CV) and chronoamperometric curves (CA) were carried out in 0.5 M H_2SO_4 containing 0.5 M methanol.

The electrochemical surface area (ECSA) was determined from the charge passed associated with the hydrogen desorption between -0.2 V to 1.2 V, and it was calculated from CVs using the followed equation:

$$\mathrm{ECSA}(m^2\ g^{-1}) = \frac{S_H / V}{10 \times 0.21(\mathrm{mC\ cm^{-2}}) \times M_{Pt}}$$

Where, S_H is the desorption peak area (A V), V is the sweep rate (V s^{-1}), the conversion value for the desorption of a hydrogen monolayer is used as 0.21 mC cm^{-2} and M_{Pt} is the mass of Pt (g).

DFT Calculation

In this study, spin polarized DFT calculations were executed using the Vienna ab-initio simulation package (VASP) with the PBE exchange correlation functional. In all the calculations, a kinetic energy cut-off of 450 eV was used to expand the electronic wave functions in the plane-wave basis. The surface Brillouin zone was sampled using (11×11×11) k-points mesh. The PtNi(111) surface was modeled with 2×2×5 supercell consisting of 17 Pt atoms and 3 Ni atoms (15 at.% of Ni). Two subsequent slabs were separated with a vacuum gap of about 20 Å. The atoms in the top three layers were allowed to relax, while the atoms in the remaining two layers were fixed at their ideal bulk positions.

The adsorption energies of O and OH were measured at 0.25 monolayer (ML) overage, respectively. It was calculated as:

$$E_{ads} = E_{adsobate+surface} - E_{adsorbbate} - E_{surface}$$

Where, $E_{adsorbate+surface}$, $E_{adsorbate}$ and $E_{surface}$ are the total energies of the species adsorption on the surface, the energy of the isolated molecule and the energy of the clean surface, respectively.

According to the results of XPS, the 15.1 at.% of Ni was detected. An fcc bulk model ($Pt_{17}Ni_3$) of suitable size was chosen, and five alloy systems were adopted, which were Pt(111) with 3 Ni atoms on the top surface ($PtNi(111)_{300}$ for short), Pt(111) with 3 Ni atoms on the subsurface ($PtNi(111)_{030}$ for short), Pt(111) with 2 Ni atom on the surface and 1 Ni atoms on the subsurface ($PtNi(111)_{210}$ for short), Pt(111) with 1 Ni atom on the surface and 2 Ni atoms on the subsurface ($PtNi(111)_{120}$ for short) and Pt(111) with three Ni atoms distributed evenly on the top 3 layers ($PtNi(111)_{111}$ for short). Moreover, Pt(111) and Ni(111) were calculated respectively as comparisons.

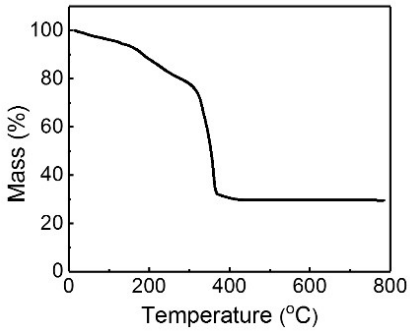

Fig. S1 TG data of the composite of meso-Pt NSs and polymer PS-P2VP-PEO.

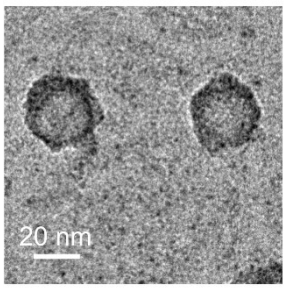

Fig. S2 TEM image of PS-P2VP-PEO micelles in the concentration of 0.4 mg mL^{-1}, in which only the PS core was highlighted by 0.1 wt% phosphotungstic acid. The diameter of PS core was measured to be *ca.* 31 nm.

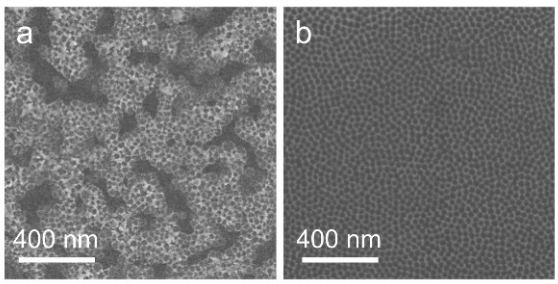

Fig. S3 Meso-Pt NSs reduced by (a) DMAB and (b) DMAB and ascorbic acid.

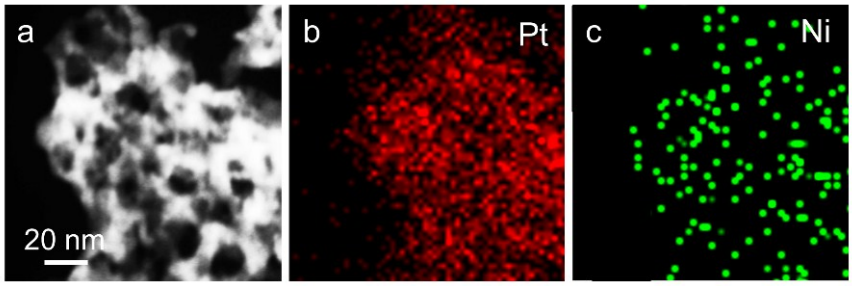

Fig. S4 (a) HAADF STEM image of meso-PtNi NSs, (b) Pt and (c) Ni element mapping images.

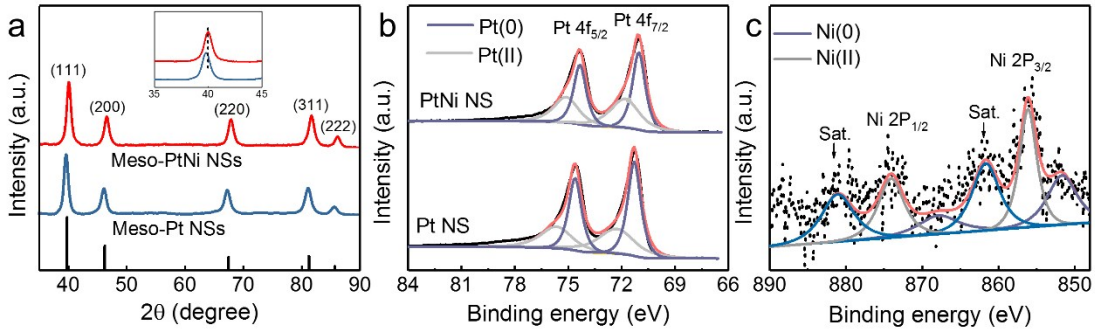

Fig. S5 (a) XRD patterns and (b) Pt 4f XPS spectra of the meso-Pt NSs and meso-PtNi NSs. (c) Ni 2p XPS spectra of meso-PtNi NSs.

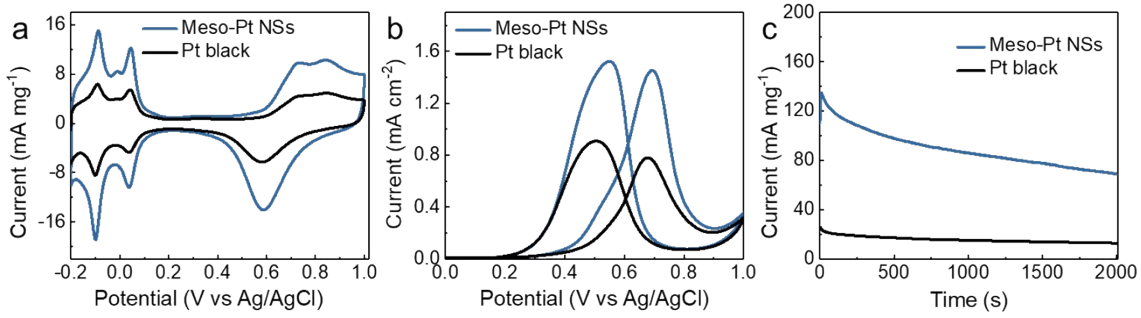

Fig. S6 (a) Cyclic voltammograms in 0.5 M H_2SO_4 at a scan rate of 50 mV·s^{-1}. (b) Specific activities of the MOR by ECSA for the recorded in a mixture of 0.5 M H_2SO_4 and 0.5 M CH_3OH at a scan rate of 50 mV s^{-1}. (c) Chronoamperometric curves for the MOR at 0.6 V.

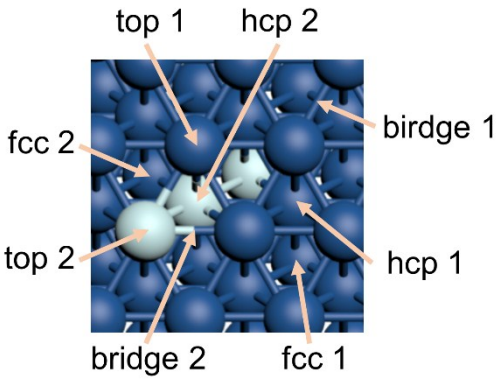

Fig. S7 Top view of the adsorption sites. There are four types of surface adsorption sites: top site, bridge site and two hollow sites (fcc and hcp). Blue spheres and white spheres represent the Pt and Ni atoms, respectively.

Table S1: Graphical comparison of specific activities of all kinds of catalysts, respectively.

Materials	The test solution	Specific activities (mA cm^{-2})	Reference
Meso-Pt NSs	0.5 M H_2SO_4 solution including 0.5 M methanol	1.45	This work
Pt nanospheres	0.5 M H_2SO_4 solution including 0.5 M methanol	1.24	[1]
Pt nanorods	0.1 M $HClO_4$ solution including 0.5 M methanol	0.45	[2]
Pt nanowires	0.5 M H_2SO_4 solution including 1 M methanol	0.98	[3]
Dendritic Pt	0.5 M H_2SO_4 solution including 0.5 M methanol	1.05	[4]

Table S2: Summary of recent reported ORR activities in 0.1 M $HClO_4$ (electrode rotating speed at 1600 rpm).

Materials	Catalyst loading (m^2 g^{-1})	LSV scan rate (mV s^{-1})	Half-wave potential (V vs. RHE)	Reference
Meso-Pt NSs	0.199	10	0.89	This work
Meso-PtNi NSs	0.199	10	0.91	This work
Graphene-wrapped PtNi nanosponge	\	10	0.89	[5]
PtNi mesoporous nanopheres	0. 142	5	0.88	[6]
PtNi nanowires	0.051	10	0.86	[7]
PtNi NPNWs	0.057	10	0.898	[8]
$Pt_5Cu_{76}Co_{11}Ni_8$ NTs	0.079	10	0.87	[9]

Table S3: Adsorption energy (eV) of OH on different PtNi alloys.

	top1	top2	bridge1	bridge2	hcp1	hcp2	fcc1	fcc2
Pt(111)	-2.51	\	-2.65	\	-1.95	\	-2.14	\
$PtNi(111)_{300}$	-2.88	\	\	\	\	\	-3.87	\
$PtNi(111)_{210}$	-2.73	\	\	-2.95	-3.29	\	\	\
$PtNi(111)_{120}$	-2.56	-2.78	-2.81	\	\	\	\	\
$PtNi(111)_{111}$	-2.54	-2.62	-2.72	-2.77	\	\	-2.71	\
Ni(111)	\	\	\	\	\	-3.02	\	-3.16

Table S4: Adsorption energy (eV) of O on different PtNi alloys.

	top1	top2	bridge1	bridge2	hcp1	hcp2	fcc1	fcc2
Pt(111)	-2.96	\	\	\	-3.92	\	-4.34	\
$PtNi(111)_{300}$	-3.59	\	\	\	-5.20	\	-5.70	\
$PtNi(111)_{210}$	\	\	\	\	-4.84	\	-5.17	\
$PtNi(111)_{120}$	\	\	\	\	-4.13	-4.23	-4.66	\
$PtNi(111)_{111}$	-4.08	-3.17	\	\	-4.26	\	-4.64	-4.16
Ni(111)	\	-3.31	\	\	\	-5.15	\	-5.26

1. Y. Li, B. P. Bastakoti, V. Malgras, C. Li, J. Tang, J. H. Kim and Y. Yamauchi, *Angew. Chem.-Int. Edit.*, 2015, **54**, 11073-11077.
2. C. L. Li, T. Sato and Y. Yamauchi, *Angew. Chem.-Int. Edit.*, 2013, **52**, 8050-8053.
3. C. Zhang, L. Xu, Y. Yan and J. Chen, *Sci. Rep.*, 2016, **6**.
4. K. Kani, M. B. Zakaria, J. J. Lin, A. A. Alshehri, J. H. Kim, Y. Bando, J. You, M. A. Hossain, J. Bo and Y. Yamauchi, *B Chem Soc Jpn*, 2018, **91**, 1333-1336.
5. Q. C. Tran, H. An, H. Ha, V. T. Nguyen, N. D. Quang, H. Y. Kim and H. S. Choi, *J. Mater. Chem. A*, 2018, **6**, 8259-8264.
6. H. J. Wang, H. J. Yu, S. L. Yin, Y. H. Li, H. R. Xue, X. N. A. Li, Y. Xu and L. Wang, *Nanoscale*, 2018, **10**, 16087-16093.
7. F. F. Chang, G. Yu, S. Y. Shan, Z. Skeete, J. F. Wu, J. Luo, Y. Ren, V. Petkov and C. J. Zhong, *J. Mater. Chem. A*, 2017, **5**, 12557-12568.
8. Y. Wang, K. Yin, L. Lv, T. Kou, C. Zhang, J. Zhang, H. Gao and Z. Zhang, *J. Mater. Chem. A*, 2017, **5**, 23651-23661.
9. L. F. Liu and E. Pippel, *Angew. Chem.-Int. Edit.*, 2011, **50**, 2729-2733.